

Glut-4 is translocated to both caveolae and non-caveolar lipid rafts, but is partially internalized through caveolae in insulin-stimulated adipocytes

Taichang Yuan^{1,2}, Shangyu Hong^{1,2}, Yao Yao^{1,2}, Kan Liao^{1,2}

¹State Key Laboratory of Molecular Biology, Institute of Biochemistry and Cell Biology, Shanghai Institutes for Biological Sciences, Chinese Academy of Sciences, Shanghai 200031, China; ²Graduate School of Chinese Academy of Sciences, 320 Yueyang Road, Shanghai 200031, China

Caveolae and non-caveolar lipid rafts are two types of membrane lipid microdomains that play important roles in insulin-stimulated glucose uptake in adipocytes. In order to ascertain their specific functions in this process, caveolae were ablated by caveolin-1 RNA interference. In Cav-1 RNAi adipocytes, neither insulin-stimulated glucose uptake nor Glut-4 (glucose transporter 4) translocation to membrane lipid microdomains was affected by the ablation of caveolae. With a modified sucrose density gradient, caveolae and non-caveolar lipid rafts could be separated. In the wild-type 3T3-L1 adipocytes, Glut-4 was found to be translocated into both caveolae and non-caveolar lipid rafts. However, in Cav-1 RNAi adipocytes, Glut-4 was localized predominantly in non-caveolar lipid rafts. After the removal of insulin, caveolae-localized Glut-4 was internalized faster than non-caveolar lipid raft-associated Glut-4. The internalization of Glut-4 from plasma membrane was significantly decreased in Cav-1 RNAi adipocytes. These results suggest that insulin-stimulated Glut-4 translocation and glucose uptake are caveolae-independent events. Caveolae play a role in the internalization of Glut-4 from plasma membrane after the removal of insulin.

Keywords: Glut-4 translocation, Glut-4 internalization, lipid rafts, caveolae, sucrose density gradient flotation

Cell Research (2007) 17:772-782. doi: 10.1038/cr.2007.73; published online 11 September 2007

Introduction

In adipocytes and striated muscle cells, the rapid increase in glucose uptake after insulin stimulation has largely been attributed to the rapid translocation of glucose transporter-4 (Glut-4) from intracellular storage vesicles to the plasma membrane [1-4]. It is reported that plasma membrane lipid microdomains are involved in this insulin-stimulated Glut-4 translocation [5-11]. To analyze the function(s) of membrane lipid microdomains in insulin-stimulated Glut-4 translocation, cholesterol-depletion reagents, such as β -methylcyclodextrin and filipin, are often used to dis-

rupt the plasma membrane microdomains [5-10]. These reagents, however, do not discriminate between lateral non-caveolar lipid rafts and invaginated caveolae, which are two different types of lipid microdomains [12-15]. Both types of lipid microdomains are abolished by the depletion of cholesterol.

Caveolin-1 is the essential structural protein of caveolae. Without this structural protein caveolae cannot be formed on the cell membrane [16]. The cells in caveolin-1 knockout mice are devoid of caveolae [16]. In our previous study, a Cav-1 RNAi 3T3-L1 cell line was generated by suppressing the expression of caveolin-1 with RNA interference [17]. Caveolae are completely ablated from the plasma membrane of the RNAi cell, whereas the glycosphingolipid-enriched membrane microdomains are not affected [17]. Thus, the functional difference between caveolae and non-caveolar lipid microdomains in insulin-stimulated Glut-4 translocation can be identified by Cav-1 RNAi 3T3-L1 adipocytes.

Correspondence: Kan Liao

Tel: +86-21-54921113; Fax: +86-21-54921011

E-mail: kliao@sibs.ac.cn

Received 29 November 2006; revised 8 February, 9 March 2007; accepted 12 March 2007; published online 11 September 2007

It is reported that translocated Glut-4 is associated with caveolin-1-enriched plasma membrane fractions after insulin stimulation [6-9, 11]. The translocated Glut-4 is also visualized in caveolar pits under the electron microscope [7, 8]. However, the intracellular Glut-4 storage vesicles that are isolated using anti-Glut-4 antibody affinity purification from non-stimulated basal adipocytes do not have detectable levels of caveolin-1 protein [18]. These observations suggest that the association of Glut-4 with caveolae is the result of Glut-4 translocation after insulin stimulation. It is possible that intracellular Glut-4 storage vesicles are fused directly with caveolae during insulin stimulation or that Glut-4 on plasma membrane migrates into caveolae after translocation. If caveolae are important for Glut-4 vesicle fusion, the ablation of caveolae in adipocytes will block or interrupt this hormone-stimulated Glut-4 translocation. Studies with Cav-1 RNAi adipocytes will be able to elucidate the function of caveolae in insulin-stimulated Glut-4 translocation.

Here we report that translocated Glut-4 is partitioned into both caveolae and non-caveolar lipid rafts. In the absence of caveolae, non-caveolar lipid rafts alone are sufficient for insulin-stimulated Glut-4 translocation and glucose uptake. It appears that non-caveolar lipid rafts are functionally sufficient in insulin signaling and Glut-4 translocation, while caveolae are important for Glut-4 internalization from plasma membrane.

Materials and Methods

Materials

Monoclonal anti-Glut-4 antibody was purchased from R&D Systems (Minneapolis, MN, USA). Anti-caveolin-1 α isoform, anti-caveolin-2, anti-insulin receptor β -subunit, anti-phosphotyrosine and anti-clathrin light-chain antibodies were from Santa Cruz Biotechnology, Inc. (Santa Cruz, CA, USA). Anti-Akt2 antibody was from Cell Signaling Technology, Inc. (Beverly, MA, USA). 2-Deoxy-D-[1- 14 C]glucose was from Amersham Biosciences UK Limited (Buckinghamshire, UK). Dulbecco's modified Eagle's medium (DMEM) and protein A-agarose were from Invitrogen. Horseradish peroxidase (HRP)-conjugated, fluorescein isothiocyanate (FITC)-conjugated or rhodamine-conjugated secondary antibodies, HRP-conjugated cholera toxin subunit B, insulin, dexamethasone, 3-isobutyl-1-methylxanthine, infinity cholesterol reagents, and poly-L-lysine were from Sigma. FITC-conjugated transferrin was from Molecular Probes, Inc. (Eugene, OR, USA).

Cell culture and differentiation induction of 3T3-L1 pre-adipocytes and Oil-Red-O staining

3T3-L1 cells were cultured and induced to differentiate following the protocol described previously [19, 20]. On day 8, differentiated 3T3-L1 adipocytes were stained with Oil-Red-O to show the triglyceride accumulation. Caveolin-1 RNAi 3T3-L1 cells were generated and characterized by Hong *et al.* [17]. They were cultured and differentiated under the same conditions as the wild-type 3T3-L1 cells.

Western immunoblot

Samples were prepared in 1 \times Laemmli SDS buffer containing 20 mM dithiothreitol. After SDS-polyacrylamide gel electrophoresis and transfer to an Immobilon-P membrane (Millipore Inc.), the target protein was revealed by immunoblotting and enhanced chemiluminescence [21].

Measurement of glucose uptake and Glut-4 endocytosis

Glucose transporter activity was measured by 2-deoxy-D-glucose uptake as described previously [22, 23]. 3T3-L1 adipocytes cultured in 35 mm dishes were serum starved with DMEM for 3 h, washed three times with warm KRH buffer (25 mM HEPES, pH 7.4, 120 mM NaCl, 5 mM KCl, 1.2 mM MgSO₄, 1.3 mM CaCl₂, 1.3 mM KH₂PO₄) and then incubated in KRH buffer at 37 °C. Subsequently, the cells were stimulated with or without 100 nM insulin for 30 min and 2-deoxy-D-[1- 14 C]glucose was added during the last 5 min at a final concentration of 50 μ M with 0.2 μ Ci/ml. Glucose uptake was terminated by washing three times with ice-cold phosphate-buffered saline (PBS). The cells were lysed with 1% SDS and subjected to liquid scintillation counting.

For kinetic analysis of glucose uptake, cells were stimulated with 100 nM insulin and 2-deoxy-D-[1- 14 C]glucose uptake was measured for 2 min periods at each indicated time point.

For Glut-4 endocytosis analysis, cells were treated with 100 nM insulin for 30 min, washed twice with low pH KRM buffer (20 mM Mes, pH 6.0, 120 mM NaCl, 5 mM KCl, 1.2 mM MgSO₄, 1.3 mM CaCl₂, 1.3 mM KH₂PO₄) and then incubated in the same washing buffer at 37 °C for 5 min to remove insulin. After washing with normal pH KRH buffer twice, the cells were incubated in KRH buffer at 37 °C. At each indicated time point, 2-deoxy-D-[1- 14 C]glucose uptake was measured for 2 min periods, or the cells were harvested for the analysis of Glut-4.

Analysis of transferrin endocytosis

Adipocytes were washed and incubated in DMEM containing 1% bovine serum albumin (BSA) for 30 min at 37 °C. FITC-conjugated transferrin (5 μ g/ml in DMEM with 1% BSA) was added to the cells. At the indicated time, cells were placed on ice, washed twice with cold acidic DMEM (pH 3.5) with 1% BSA and four times with cold PBS to remove surface-bound transferrin. The cells were then subjected to flow cytometry analysis to establish the fluorescence intensity of FITC.

Preparation of a plasma membrane lawn and immunofluorescence staining analysis

3T3-L1 pre-adipocytes were cultured on coverslips that were pre-treated with 0.5 mg/ml poly-L-lysine and differentiated into adipocytes. Cells were serum starved for 3 h and then treated with or without 100 nM insulin for 30 min. The plasma membrane lawns were prepared as described by Robinson and James [24]. The membrane sheets attached on the coverslips were fixed in 4% paraformaldehyde for 20 min, washed, blocked with 1% BSA and then incubated with primary antibodies [anti-Cav-1 antibody (rabbit) and anti-Glut-4 antibody (mouse)] and secondary antibodies (rhodamine-conjugate anti-rabbit and FITC-conjugate anti-mouse). The plasma membrane lawns were visualized using a confocal microscope.

For immunofluorescence staining of intact cells, adipocytes were permeabilized with 0.2% Triton X-100 in PBS for 10 min after fixation. The staining process was the same as described in the previous

paragraph.

Isolation of plasma membrane, extraction of sodium carbonate and sucrose density gradient centrifugation of membrane lipid microdomains

Cells were serum starved for 3 h, stimulated with or without 100 nM insulin for 30 min, washed with cold HES buffer (20 mM HEPES, pH 7.4, 1 mM EDTA, 0.25 M sucrose) three times and homogenized in the same HES buffer plus the protease inhibitor cocktails 1 and 2 [25]. The cell lysate was centrifuged at $16\,000 \times g$ for 20 min at 4 °C and the membrane pellet was re-suspended in HES buffer. Plasma membrane was isolated by loading the re-suspended membrane pellet onto a 1.12 M sucrose cushion and centrifuged at $100\,000 \times g$ for 60 min [26]. The membrane fraction on the density interface was collected, diluted with 20 mM HEPES, pH 7.4 and 1 mM EDTA solution and pelleted by centrifugation.

The plasma membrane preparation was re-suspended in 2 ml 0.5 M Na_2CO_3 , pH 11.0, sonicated, mixed with 2 ml 90% sucrose in 0.15 M NaCl and 25 mM Mes solution, placed at the bottom of an SW41

centrifuge tube, overlain with 4 ml 35% sucrose and 4 ml 5% sucrose in a sodium carbonate solution (0.25 M Na_2CO_3 , pH 11.0, 0.15 M NaCl and 25 mM Mes). The gradient was centrifuged at $180\,000 \times g$ for 20 h in an SW41 rotor [27]. Fractions were collected from the top of the gradient and proteins were analyzed through western blotting. The glycosphingolipid was analyzed with HRP-conjugate cholera toxin subunit B as described by Hong *et al.* [17].

A four-layer sucrose density gradient was developed in our laboratory to separate caveolin-enriched membrane microdomains from other insoluble membrane lipid microdomains. The density gradient of 4 ml 45% sucrose, 2 ml 35% sucrose, 4 ml 20% sucrose and 2 ml 5% sucrose in the sodium carbonate solution was formed in a 14 × 89 mm Beckman centrifuge tube and centrifuged at $180\,000 \times g$ for 20 h in an SW41 rotor. 0.5 ml fractions were collected from the top of the gradient.

Analysis of insulin receptor autophosphorylation

Insulin stimulation was the same as described in the previous sections. At each indicated time point, cells were washed with cold

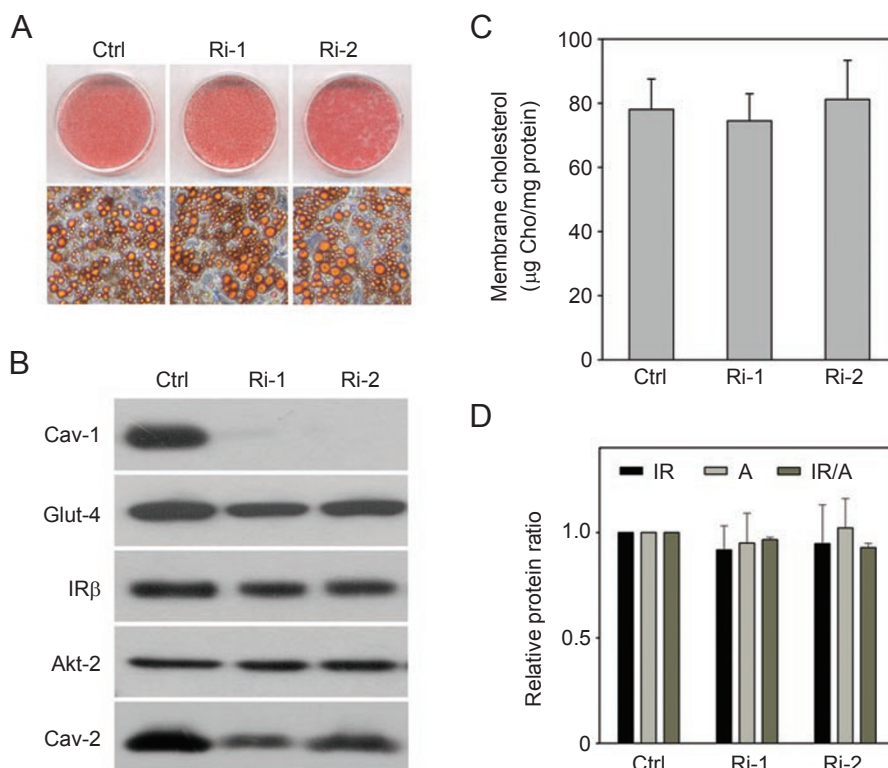


Figure 1 Characterization of Cav-1 RNAi adipocytes. **(A)** Oil-Red-O staining of adipocytes. Ctrl, wild-type 3T3-L1 adipocytes on day 8 after differentiation induction; Ri-1 and Ri-2, two independent cell lines of Cav-1 RNAi 3T3-L1 adipocytes on day 8 after differentiation induction. **(B)** Western blot analysis of proteins in wild-type and Cav-1 RNAi adipocytes. Cav-1, Glut-4, IR β , Akt-2 and Cav-2 indicate caveolin-1, glucose transporter 4, insulin receptor β subunit, protein kinase B/Akt 2 and caveolin-2 respectively. **(C)** Cholesterol content in the plasma membrane of wild-type and Cav-1 RNAi adipocytes. The plasma membrane was isolated as described in the Materials and Methods. Cholesterol content is expressed as the ratio of cholesterol to the plasma membrane proteins. **(D)** Relative ratio of insulin receptor in Cav-1 RNAi cells and wild-type cells. The protein amount of insulin receptor (IR) and actin (A) was determined by densitometry scanning of protein bands on western blot and normalized with the amount of actin (IR/A). The ratio between Cav-1 RNAi cells and wild-type cells in three experiments was averaged.

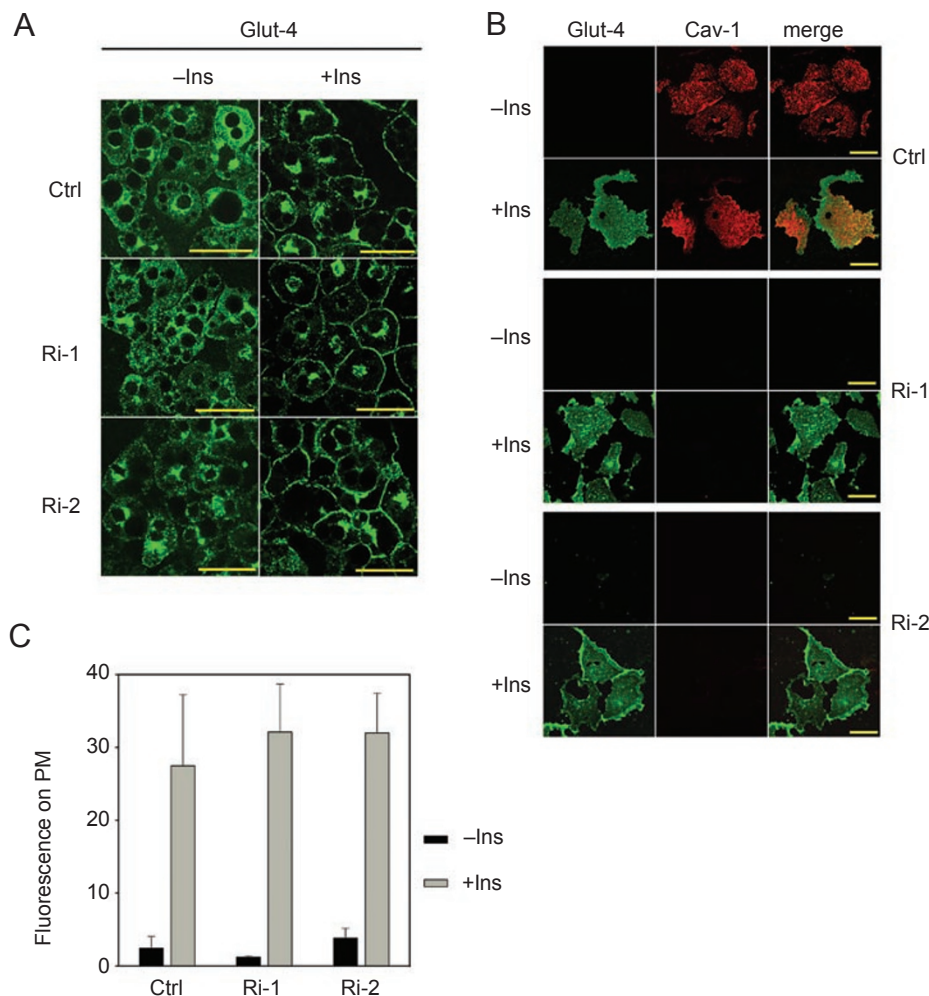


Figure 2 Immunofluorescence staining of Glut-4 in 3T3-L1 adipocytes and Cav-1 RNAi adipocytes. **(A)** A confocal microscope image of day 8 adipocytes stained with anti-Glut-4 antibody. Bar = 40 μ M. Day 8 adipocytes were treated with 100 nM insulin for 30 min (+Ins) or without (-Ins). They were stained with anti-Glut-4 antibody (Glut-4). Ctrl, Ri-1 and Ri-2 are the same as in **Figure 1A**. **(B)** Plasma membrane sheets double-stained with anti-caveolin-1 and anti-Glut-4 antibodies. Bar = 20 μ M. The plasma membrane lawn was prepared as described in the Materials and Methods from day 8 adipocytes that were treated with 100 nM insulin for 30 min (+Ins) or without (-Ins). Glut-4, FITC fluorescence of anti-Glut-4 antibody; Cav-1, rhodamine fluorescence of anti-caveolin-1 antibody; merge, overlapped image. **(C)** Fluorescence intensity of Glut-4 on the plasma membrane. The fluorescence intensity of Glut-4 on the plasma membrane sheets (fluorescence on PM) was determined by confocal microscopy (using the fluorescence intensity/pixel area). The fluorescence intensity of eight membrane sheets was averaged.

PBS and lysed in an immunoprecipitation buffer (1% Triton X-100, 50 mM HEPES, pH 7.4, 2.5 mM EDTA, 150 mM NaCl, 30 mM β -glycerophosphate, 1 mM sodium vanadate, 1 mM PMSF and 2 μ l/ml protease inhibitor cocktails 1 and 2). The cell lysate was homogenized and extracted at 4 $^{\circ}$ C for 1 h. After centrifugation at 12 000 \times g for 15 min, the supernatant (500 μ g protein) was mixed with 1 μ g anti-insulin receptor β -subunit antibody for 2 h at 4 $^{\circ}$ C and then with protein A-agarose overnight at 4 $^{\circ}$ C. The protein A-agarose beads were collected, washed and re-suspended in 1 \times Laemmli SDS sample buffer for western blot analysis.

For insulin sensitivity analysis, serum-starved 3T3-L1 adipocytes

were treated with insulin at the indicated concentration for 10 min.

Measurement of plasma membrane cholesterol

Plasma membrane was prepared as described in the previous section. Cholesterol in isolated plasma membrane was extracted with isopropanol and measured using the infinity cholesterol reagents kit.

Results

Glut-4 translocation in Cav-1 RNAi adipocytes

Cav-1 RNAi 3T3-L1 cells were previously generated in our laboratory and characterized [17]. Except for caveolae, these Cav-1 RNAi cells exhibited no difference from the wild-type cells or the shuffled-sequence RNAi control cells [17]. It appeared that in the absence of Cav-1, the residual Cav-2 was not sufficient to form an invaginated caveolar structure [17] (Figure 1B). Under standard hormone induction, these cells differentiated into adipocytes (Figure 1A). Morphologically, Cav-1 RNAi adipocytes and wild-type 3T3-L1 adipocytes were the same (Figure 1A). In addition, no change in the expression of insulin receptor, Glut-4 and protein kinase B/Akt2 was detected in Cav-1 RNAi adipocytes, neither was the cholesterol content in plasma membrane (Figure 1B-1D).

Intracellular Glut-4 vesicles are translocated to plasma membrane when stimulated by insulin. This vesicle translocation process can be visualized with Glut-4 immunofluorescence staining (Figure 2A). In the quiescent adipocytes, only the cytoplasm was stained by anti-Glut-4 antibody (Figure 2A). After insulin stimulation, however, most anti-Glut-4 antibody staining was on the plasma membrane. Similar results were observed in Cav-1 RNAi adipocytes (Figure 2A). It is clear that the lack of caveolae did not reduce the translocation of intracellular Glut-4 vesicles to plasma membrane.

The Glut-4 translocation in Cav-1 RNAi adipocytes was further confirmed by double immunostaining with anti-Glut-4 and anti-Cav-1 antibodies on the isolated plasma membrane sheets. Without stimulation the isolated plasma membrane sheets of Cav-1 RNAi adipocytes were stained by neither antibody, whereas the membrane sheets of the wild-type 3T3-L1 adipocytes were stained by caveolin-1 antibody (Figure 2B). With insulin stimulation, the plasma membrane sheets of both adipocytes were stained by Glut-4 antibody (Figure 2B). The quantitative analysis of Glut-4 fluorescence intensity on plasma membrane after insulin stimulation showed a similar Glut-4 translocation in both wild-type and Cav-1 RNAi adipocytes (Figure 2C). These results indicate that without caveolae the translocated Glut-4 could still stay in the plasma membrane.

Glucose uptake in Cav-1 RNAi adipocytes

To confirm that the translocated Glut-4 in Cav-1 RNAi adipocytes is functional, the glucose uptake by Cav-1 RNAi adipocytes was measured. As indicated in Figure 3A, the maximum glucose uptake rates after insulin stimulation in both wild type and Cav-1 RNAi adipocytes were the same. This observation is consistent with the result of Glut-4 protein translocation (Figure 2C). Without caveolae, Glut-4 on plasma membrane was fully functional for transporting glucose.

During the initial response to insulin stimulation, there

was a lag in the increase of glucose uptake activity in the wild-type 3T3-L1 adipocytes (Figure 3B). In comparison, this initial lag of response to insulin was not detected in Cav-1 RNAi adipocytes (Figure 3B). There is a statistical difference in the initial response to insulin stimulation between Cav-1 RNAi adipocytes and the wild-type adipocytes (Figure 3B). This difference in initial glucose uptake activity does not result from the increased insulin sensitivity in Cav-1 RNAi adipocytes, since no difference in insulin-activated receptor tyrosine autophosphorylation was detected between these two adipocytes (Figure 3C and 3D). This conclusion was further supported by our previous study with Cav-1 RNAi cells [17]. In response to insulin, the tyrosine phosphorylation of insulin receptor substrate-1 and the activation of protein kinase B/Akt-1 or ERK were the same as in both wild-type and Cav-1 RNAi cells [17]. In addition, insulin receptor signaling is reported to be independent from caveolin-1 and caveolae [28-30].

Internalization of Glut-4 through caveolae

It has been reported that the caveolin organization is necessary for Glut-4 endocytosis [31]. Thus, in Cav-1 RNAi adipocytes, Glut-4 internalization from plasma membrane should be blocked or decreased. Consequently, the down-regulation of glucose uptake activity after the removal of insulin would be inhibited.

Cellular endocytosis is carried out by both clathrin-coated pits and caveolae. In Cav-1 RNAi adipocytes, the blockade of caveolae-mediated endocytosis should not affect clathrin-coated, pit-mediated endocytosis. To measure clathrin-coated, pit-mediated endocytosis, transferrin endocytosis was analyzed [32-34]. As shown in Figure 4A and 4B, the internalization of transferrin in both wild-type and Cav-1 RNAi adipocytes were the same.

After the removal of insulin, Glut-4 on plasma membrane is gradually internalized and glucose uptake activity is downregulated. The residual glucose uptake activity in Cav-1 RNAi adipocytes after washing away of insulin is two- to three-folds of that in the wild-type adipocytes (Figure 4C). Kinetic analysis showing a clear decrease in glucose uptake activity suggests a much slower internalization of Glut-4 in Cav-1 RNAi adipocytes than in wild-type adipocytes (Figure 4D). At 4 h after washing away of insulin, the residual glucose uptake in Cav-1 RNAi cells was about 17% of the maximal rate (result not shown). This residual rate in Cav-1 RNAi cells was similar to the residual glucose uptake rate in the wild-type cells at 2 h after the removal of insulin. This higher residual glucose uptake activity in Cav-1 RNAi adipocytes was further substantiated by the greater retention of Glut-4 protein on plasma membrane (Figure 4E). Thirty minutes after washing away the insulin, much higher Glut-4 retention in

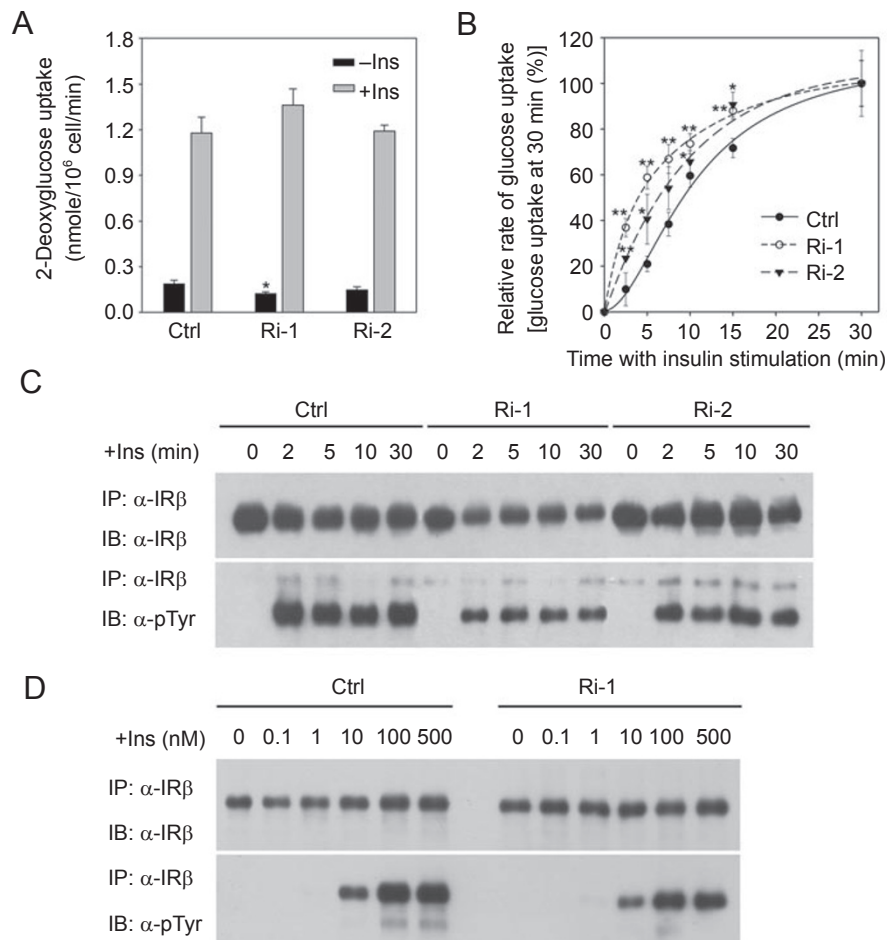


Figure 3 Glucose uptake and insulin receptor activation in Cav-1 RNAi adipocytes. **(A)** Insulin-stimulated glucose uptake in Cav-1 RNAi adipocytes. Adipocytes were treated with 100 nM insulin for 30 min and glucose uptake was measured by 2-deoxy- ^{14}C -glucose internalization. Student's *t*-test was performed between RNAi cells and wild-type cells. **p* < 0.05. **(B)** The kinetics of glucose uptake activity after insulin stimulation. Adipocytes were treated with 100 nM insulin. Three independent measurements were averaged. **p* < 0.05; ***p* < 0.01. **(C)** Insulin-stimulated receptor autophosphorylation. Membrane proteins were extracted with Triton X-100 from adipocytes. The insulin receptor β -subunit was immunoprecipitated (IP) with anti-insulin receptor β -subunit antibody (α -IR β) and blotted (IB) with anti-phospho-tyrosine antibody (α -PTyr). 0, 2, 5, 10 and 30 min indicate the times of insulin treatment. **(D)** Insulin receptor sensitivity. The labels are the same as in panel (C). 0, 0.1, 1, 10, 100 and 500 nM indicate the insulin concentrations.

plasma membrane of Cav-1 RNAi adipocytes was observed (Figure 4F). Glut-4 internalization was clearly reduced in the absence of caveolae-mediated endocytosis. As a control, the amount of insulin receptor in plasma membrane remained constant in both Cav-1 RNAi adipocytes and wild-type adipocytes (Figure 4E).

Translocation of Glut-4 to non-caveolar lipid rafts as well as caveolae in plasma membrane

In Cav-1 RNAi adipocytes, the lack of caveolae did not prevent Glut-4 translocation (Figures 2 and 3). However, in several studies it is reported that translocated Glut-4 was

localized in caveolae [5-11]. If caveolae were essential for Glut-4 localization in plasma membrane, the localization of Glut-4 in plasma membrane of Cav-1 RNAi adipocytes should be resolved.

To analyze the localization of Glut-4 in plasma membrane of Cav-1 RNAi adipocytes, membrane lipid microdomains were isolated from the purified plasma membrane. As shown in Figure 5A, in insulin-stimulated wild-type adipocytes, the translocated Glut-4 was co-fractionated with caveolar membrane fractions. Interestingly, Glut-4 in Cav-1 RNAi adipocytes was still co-fractionated with membranes corresponding to caveolar fractions (Figure

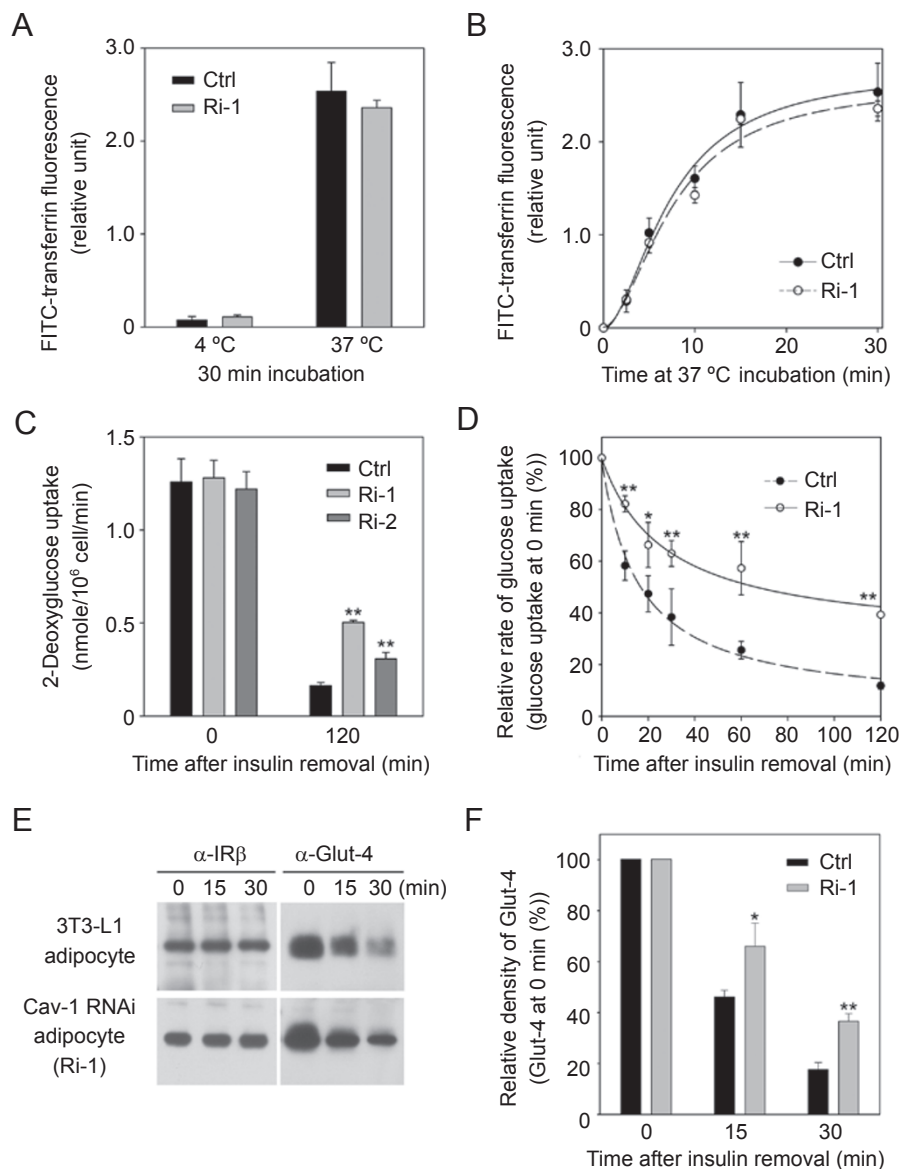


Figure 4 Internalization of Glut-4 in 3T3-L1 adipocytes and Cav-1 RNAi adipocytes. **(A)** Internalization of transferrin in adipocytes. Incubation of FITC-transferrin with cells was at 4 °C or 37 °C. **(B)** The time course of transferrin internalization. **(C)** Glucose uptake in adipocytes after the removal of insulin. Insulin was washed away from the adipocytes after a 30-min insulin treatment as described in the Materials and Methods section. Glucose uptake activity was measured at 0 and 120 min after washing. The results are the average of three experiments. $**p < 0.01$. **(D)** The rate of decrease of glucose uptake activity after the removal of insulin. Glucose uptake was measured at the indicated time points after the removal of insulin. $*p < 0.05$; $**p < 0.01$. **(E)** Residual Glut-4 on the plasma membrane after the removal of insulin. The plasma membrane was isolated at the indicated time points (0, 15 and 30 min) after the removal of insulin. The proteins were blotted with anti-insulin receptor β -subunit antibody (α -IR β) and anti-Glut-4 antibody (α -Glut-4). **(F)** Relative Glut-4 density on a western blot **(E)**. The results of three experiments were averaged. $*p < 0.05$; $**p < 0.01$.

5A). In both adipocytes, insulin receptor, flotillin-1, Glut-4 and glycosphingolipids were co-fractionated regardless to the presence of caveolin-1 or not (Figure 5A).

The localization of Glut-4 in membrane lipid microdo-

mains in Cav-1 RNAi adipocytes raised the possibility that Glut-4 was translocated to non-caveolar lipid rafts as well as caveolae. With four-layer sucrose density gradient flotation (see Materials and Methods for details), two membrane

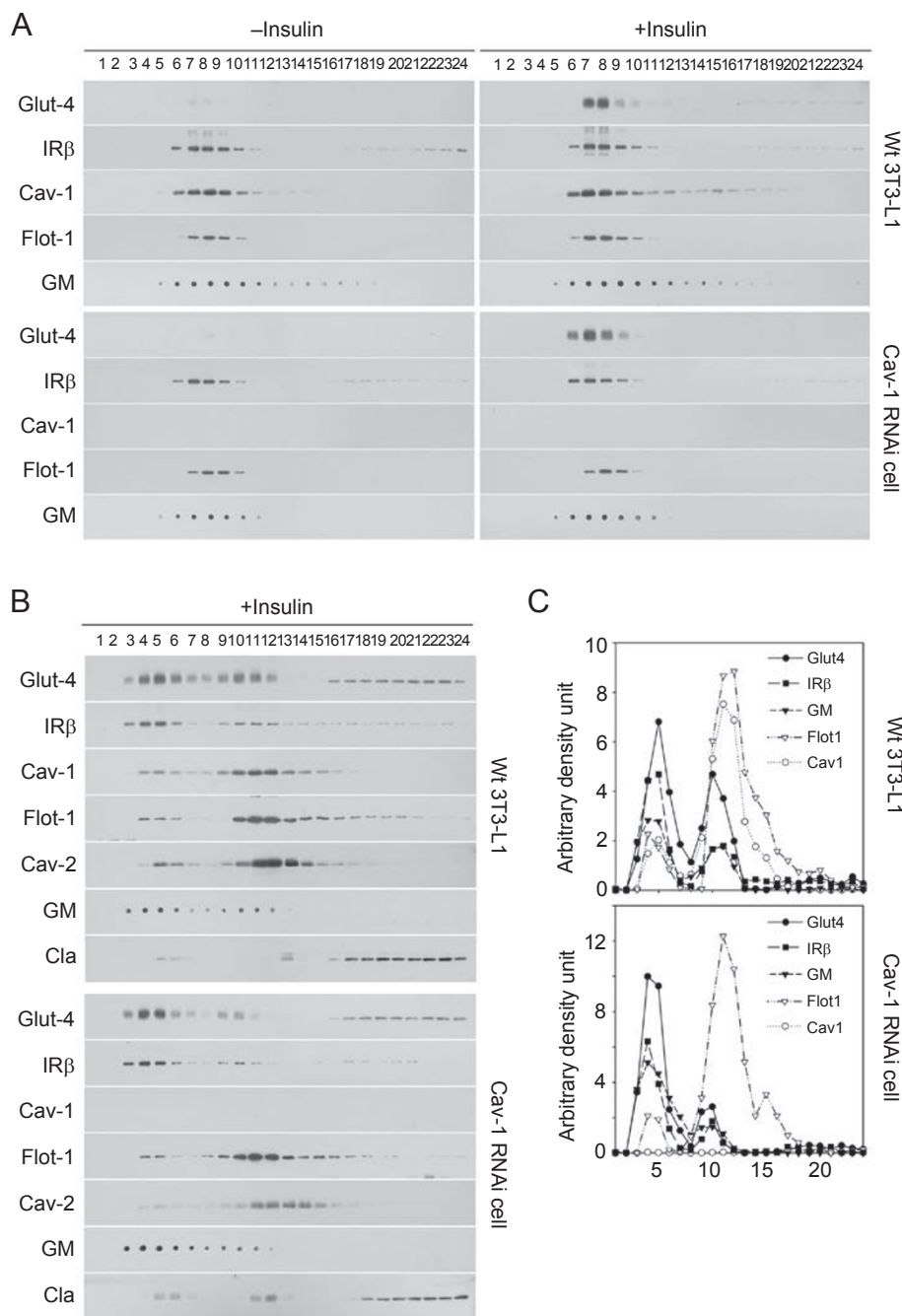


Figure 5 Insulin-stimulated Glut-4 translocation to non-caveolar membrane lipid microdomains in Cav-1 RNAi adipocytes and 3T3-L1 adipocytes. **(A)** Insulin-stimulated Glut-4 translocation to membrane lipid microdomains in the plasma membrane. The plasma membrane was isolated from adipocytes treated with insulin or not. The membrane lipid microdomains were separated by sucrose density gradient flotation in sodium carbonate solution as described in the Materials and Methods. The proteins in density gradient fractions were detected using western blot analysis with antibodies against Glut-4 (Glut-4), insulin receptor β -subunit (IR β), caveolin-1 (Cav-1) and flotillin-1 (Flot-1). The glycosphingolipids (GM) in each fraction were detected by dot-blot with horse-radish peroxidase cholera toxin conjugate. -Insulin, cells without insulin stimulation; +Insulin, cells treated with 100 nM insulin for 30 min; 1, 2, to 24, the fractions of sucrose density gradient flotation with 1 at the top of the gradient and 24 at the bottom. **(B)** Glut-4 translocation to non-caveolar membrane lipid microdomains. Plasma membranes were isolated from 3T3-L1 adipocytes and Cav-1 RNAi adipocytes were treated with insulin. Non-caveolar membrane microdomains and caveolae were separated with a modified four-layer sucrose density gradient flotation as described in the Materials and Methods. Cav-2 and Cla, western blot analysis with anti-caveolin-2 antibody and anti-clathrin antibody respectively. All the other labels are the same as in panel (A). **(C)** Density scanning for the protein bands from the western blot (B).

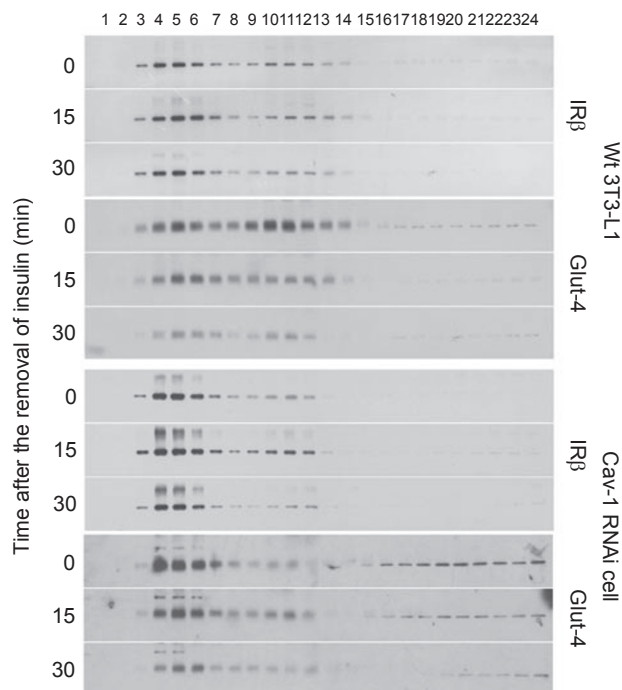


Figure 6 Residual Glut-4 in membrane lipid microdomains after the removal of insulin. Insulin was washed away after a 30 min treatment as described in Materials and Methods. At the indicated time points (0, 15, 30 min), plasma membrane was isolated and lipid microdomains were separated using the modified sucrose density flotation. Samples from each fraction were blotted with anti-insulin receptor β -subunit (IR β) and anti-Glut-4 (Glut-4) respectively.

lipid microdomain fractions were isolated as indicated by glycosphingolipid enrichment (Figure 5B). In these two glycosphingolipid-enriched insoluble membrane fractions, caveolin-1 and flotillin-1 were predominantly fractionated into the heavy insoluble membrane fraction while insulin receptor was mostly partitioned into the light insoluble membrane fraction (Figure 5B and 5C). Thus, the heavy glycosphingolipid enriched insoluble membrane contains caveolae and the light glycosphingolipid enriched insoluble membrane contains non-caveolar lipid rafts.

In wild-type adipocytes, the translocated Glut-4 was present in both insoluble membrane fractions (Figure 5B and 5C). In fact, more Glut-4 was localized in non-caveolar lipid rafts than caveolae (Figure 5C). The presence of Glut-4 in non-caveolar lipid rafts was further confirmed by Cav-1 RNAi adipocytes. In the absence of caveolae, almost all Glut-4 was fractionated into non-caveolar lipid rafts (Figure 5B). Although there was some residual Cav-2 protein in Cav-1 RNAi cells, it was not co-fractionated with Glut-4 (Figure 5B). As a control, clathrin, which is not a membrane lipid microdomain protein, was fractionated in

the bottom of the gradient (Figure 5B).

With this modified density gradient, the internalization of Glut-4 localized in caveolae and non-caveolar lipid rafts could be analyzed separately. As shown in Figure 6, after washing away of insulin, Glut-4 was internalized faster in caveolae than in non-caveolar lipid rafts. Very little Glut-4 was localized in the membrane fractions corresponding to the caveolar membrane in Cav-1 RNAi adipocytes and no significant internalization of Glut-4 from these fractions was observed (Figure 6). The reduced Glut-4 internalization in Cav-1 RNAi adipocytes can most likely be attributed to the lack of caveolae-mediated endocytosis.

Discussion

Insulin-stimulated glucose uptake includes several steps: insulin receptor activation, receptor signal transduction, intracellular Glut-4 translocation and glucose uptake by the translocated Glut-4. Caveolae have been reported to be involved in these events [5-11]. However, the functional analysis of caveolae has always been complicated by the presence of non-caveolar membrane lipid rafts [12-15, 35-38]. In fact, Glut-4 was found to be partitioned into both caveolae and non-caveolar lipid rafts (Figure 5). This observation suggested the functional overlap or replacement between caveolae and non-caveolar lipid rafts in glucose uptake. The results from Cav-1 RNAi adipocytes clearly support this hypothesis. Instead of partitions between caveolae and non-caveolar lipid rafts, almost all the translocated Glut-4 was localized in non-caveolar lipid rafts in cells without caveolae (Figure 5B) and no adversary effect on insulin-stimulated Glut-4 translocation and glucose uptake was observed (Figures 2-4).

Although Cav-1^{-/-} mice on a normal diet display some disorders in lipid metabolism, such as elevated levels of free fatty acids and triglycerides and decreased expression of leptin and ACRP30, there are no changes in insulin, glucose and cholesterol levels [39, 40]. However, insulin sensitivity in Cav-1^{-/-} mice is decreased [40]. Since lipid metabolism and glucose metabolism are the two most important energy metabolism systems in animals, the possibility that the abnormal lipid metabolism affects the glucose metabolism in Cav-1^{-/-} mice cannot be ruled out. Unlike the situation in Cav-1^{-/-} mice, the glucose metabolism in Cav-1 RNAi adipocytes represents an isolated cellular system. In a fixed culture condition, only the direct interaction between caveolin-1 or caveolae with the glucose transporter and insulin signaling system would lead to changes in the cellular glucose metabolism.

The translocated Glut-4 in plasma membrane was observed in caveolae by electron microscopy [7, 8]. Our results indicate that Glut-4 in caveolae is not necessary

for its function but only for its internalization (Figures 4 and 6). The accumulation of Glut-4 in plasma membrane results from the balance of Glut-4 translocation and internalization. During the initial phase of insulin stimulation, the influx of Glut-4 to the plasma membrane was relatively low. Therefore, the effect on the accumulation of Glut-4 by the absence of caveolae-mediated endocytosis in Cav-1 RNAi cells was more measurable, compensating for the initial lag of glucose uptake (Figure 3B). When the cell is fully stimulated, endocytosis would be outweighed by the influx of Glut-4, which determines the maximal rate of glucose uptake.

Many cellular functions of membrane lipid microdomains have not been differentiated among the subtypes of lipid microdomains. Our current study with Cav-1 RNAi adipocytes indicates the importance for differentiating the types of membrane microdomains. The separation of caveolin-1-enriched membranes from non-caveolar glycosphingolipid-enriched membranes suggests that caveolae and non-caveolar lipid rafts have different densities (Figure 5). However, the co-fractionation of another lipid microdomain marker protein, flottilin-1, with fractions enriched with caveolin-1 suggests a heterogeneity in non-caveolar membrane lipid microdomains (Figure 5B). This flottilin-marked lipid microdomain was independent from caveolae as well as other glycosphingolipid-enriched membranes. In addition, the residual Cav-2 in Cav-1 RNAi cell was still fractionated into “caveolar” membranes even though there was no visible invaginated caveolae in plasma membrane. These observations suggest that membrane lipid microdomains are a group of heterogeneous membrane structures.

Cholesterol is an essential component in the plasma membrane of mammalian cells. Although caveolin-1 is involved in cellular cholesterol trafficking [15], Cav-1^{-/-} mice are generally healthy [16]. The results from knockout mice indicate that the function of caveolin-1 in cellular cholesterol trafficking can be compensated for by other mechanisms. In our current study with Cav-1 RNAi cells, membrane cholesterol was also not changed by the lack of caveolin-1 (Figure 1C). Apparently, other proteins or cellular mechanisms are involved in maintaining the cholesterol balance.

Acknowledgments

This work was supported by the National Natural Sciences Foundation of China (Nos. 90208007 and 30521005) and the Ministry of Science and Technology of China (No. 2002CB513000).

References

- 1 Watson RT, Kanzaki M, Pessin JE. Regulated membrane trafficking of the insulin-responsive glucose transporter 4 in adipocytes. *Endocr Rev* 2004; **25**:177-204.
- 2 Bryant NJ, Govers R, James DE. Regulated transport of the glucose transporter Glut-4. *Nat Rev Mol Cell Biol* 2002; **3**:267-277.
- 3 Watson RT, Pessin JE. Subcellular compartmentalization and trafficking of the insulin-responsive glucose transporter, Glut-4. *Exp Cell Res* 2001; **271**:75-83.
- 4 Simpson F, Whitehead JP, James DE. Glut-4—at the cross roads between membrane trafficking and signal transduction. *Traffic* 2001; **2**:2-11.
- 5 Chamberlain LH, Gould GW. The vesicle- and target-SNARE proteins that mediate Glut4 vesicle fusion are localized in detergent-insoluble lipid rafts present on distinct intracellular membranes. *J Biol Chem* 2002; **277**:49750-49754.
- 6 Ros-Baro A, Lopez-Iglesias C, Peiro S, *et al.* Lipid rafts are required for Glut-4 internalization in adipose cells. *Proc Natl Acad Sci USA* 2001; **98**:12050-12055.
- 7 Gustavsson J, Parpal S, Karlsson M, *et al.* Localization of the insulin receptor in caveolae of adipocyte plasma membrane. *FASEB J* 1999; **13**:1961-1971.
- 8 Karlsson M, Thorn H, Parpal S, Stralfors P, Gustavsson J. Insulin induces translocation of glucose transporter Glut-4 to plasma membrane caveolae in adipocytes. *FASEB J* 2002; **16**:249-251.
- 9 Parpal S, Karlsson M, Thorn H, Stralfors P. Cholesterol depletion disrupts caveolae and insulin receptor signaling for metabolic control via insulin receptor substrate-1, but not for mitogen-activated protein kinase control. *J Biol Chem* 2001; **276**:9670-9678.
- 10 Watson RT, Shigematsu S, Chiang SH, *et al.* Lipid raft microdomain compartmentalization of TC10 is required for insulin signaling and Glut-4 translocation. *J Cell Biol* 2001; **154**:829-840.
- 11 Scherer PE, Lisanti MP, Baldini G, *et al.* Induction of caveolin during adipogenesis and association of Glut-4 with caveolin-rich vesicles. *J Cell Biol* 1994; **127**:1233-1243.
- 12 Kurzchalia TV, Parton RG. Membrane microdomains and caveolae. *Curr Opin Cell Biol* 1999; **11**:424-431.
- 13 Parton RG. Cell biology. Life without caveolae. *Science* 2001; **293**:2404-2405.
- 14 Galbiati F, Razani B, Lisanti MP. Emerging themes in lipid rafts and caveolae. *Cell* 2001; **106**:403-411.
- 15 Fielding CJ, Fielding PE. Relationship between cholesterol trafficking and signaling in rafts and caveolae. *Biochim Biophys Acta* 2003; **1610**:219-228.
- 16 Drab M, Verkade P, Elger M, *et al.* Loss of caveolae, vascular dysfunction, and pulmonary defects in caveolin-1 gene-disrupted mice. *Science* 2001; **293**:2449-2452.
- 17 Hong S, Huo H, Xu J, Liao K. Insulin-like growth factor-1 receptor signaling in 3T3-L1 adipocyte differentiation requires lipid rafts but not caveolae. *Cell Death Differ* 2004; **11**:714-723.
- 18 Kandror KV, Stephens JM, Pilch PF. Expression and compartmentalization of caveolin in adipose cells: coordinate regulation with and structural segregation from Glut-4. *J Cell Biol* 1995; **129**:999-1006.
- 19 Mackall JC, Student AK, Polakis SE, Lane MD. Induction of lipogenesis during differentiation in a “preadipocyte” cell line. *J Biol Chem* 1976; **251**:6462-6464.

- 20 Jin S, Zhai B, Qiu Z, *et al.* c-Crk, a substrate of the insulin-like growth factor-1 receptor tyrosine kinase, functions as an early signal mediator in the adipocyte differentiation process. *J Biol Chem* 2000; **275**:34344-34352.
- 21 Qiu Z, Wei Y, Chen N, *et al.* DNA synthesis and mitotic clonal expansion is not a required step for 3T3-L1 preadipocyte differentiation into adipocytes. *J Biol Chem* 2001; **276**:11988-11995.
- 22 Frost SC, Lane MD. Evidence for the involvement of vicinal sulfhydryl groups in insulin-activated hexose transport by 3T3-L1 adipocytes. *J Biol Chem* 1985; **260**:2646-2652.
- 23 Tamori Y, Kawanishi M, Niki T, *et al.* Inhibition of insulin-induced Glut-4 translocation by Munc18c through interaction with syntaxin4 in 3T3-L1 adipocytes. *J Biol Chem* 1998; **273**:19740-19746.
- 24 Robinson LJ, James DE. Insulin-regulated sorting of glucose transporters in 3T3-L1 adipocytes. *Am J Physiol* 1992; **263**:E383-E393.
- 25 Ronnett GV, Knutson VP, Kohanski RA, Simpson TL, Lane MD. Role of glycosylation in the processing of newly translated insulin proreceptor in 3T3-L1 adipocytes. *J Biol Chem* 1984; **259**:4566-4575.
- 26 Simpson IA, Yver DR, Hissin PJ, *et al.* Insulin-stimulated translocation of glucose transporters in the isolated rat adipose cells: characterization of subcellular fractions. *Biochim Biophys Acta* 1983; **763**:393-407.
- 27 Song KS, Li S, Okamoto T, *et al.* Co-purification and direct interaction of Ras with caveolin, an integral membrane protein of caveolae microdomains. Detergent-free purification of caveolae microdomains. *J Biol Chem* 1996; **271**:9690-9697.
- 28 Souto RP, Vallega G, Wharton J, *et al.* Immunopurification and characterization of rat adipocyte caveolae suggest their dissociation from insulin signaling. *J Biol Chem* 2003; **278**:18321-18329.
- 29 Wharton J, Meshulam T, Vallega G, Pilch P. Dissociation of insulin receptor expression and signaling from caveolin-1 expression. *J Biol Chem* 2005; **280**:13483-13486.
- 30 Gonzalez E, Nagiel A, Lin AJ, Golan DE, Michel T. Small interfering RNA-mediated down-regulation of caveolin-1 differentially modulates signaling pathways in endothelial cells. *J Biol Chem* 2004; **279**:40659-40669.
- 31 Shigematsu S, Watson RT, Khan AH, Pessin JE. The adipocyte plasma membrane caveolin functional/structural organization is necessary for the efficient endocytosis of Glut-4. *J Biol Chem* 2003; **278**:10683-10690.
- 32 Harding C, Heuser J, Stahl P. Receptor-mediated endocytosis of transferrin and recycling of the transferrin receptor in rat reticulocytes. *J Cell Biol* 1983; **97**:329-339.
- 33 Hanover JA, Willingham MC, Pastan I. Kinetics of transit of transferrin and epidermal growth factor through clathrin-coated membranes. *Cell* 1984; **39**:283-293.
- 34 Lamaze C, Baba T, Redelmeier TE, Schmid SL. Recruitment of epidermal growth factor and transferrin receptors into coated pits *in vitro*: differing biochemical requirements. *Mol Biol Cell* 1993; **4**:715-727.
- 35 Anderson RG. The caveolae membrane system. *Annu Rev Biochem* 1998; **67**:199-225.
- 36 Simons K, Ikonen E. Functional rafts in cell membranes. *Nature* 1997; **387**:569-572.
- 37 Brown DA, London E. Functions of lipid rafts in biological membranes. *Annu Rev Cell Dev Biol* 1998; **14**:111-136.
- 38 Simons K, Toomre D. Lipid rafts and signal transduction. *Nat Rev Mol Cell Biol* 2000; **1**:31-39.
- 39 Razani B, Combs TP, Wang XB, *et al.* Caveolin-1-deficient mice are lean, resistant to diet-induced obesity, and show hypertriglyceridemia with adipocyte abnormalities. *J Biol Chem* 2002; **277**:8635-8647.
- 40 Cohen AW, Razani B, Wang XB, *et al.* Caveolin-1-deficient mice show insulin resistance and defective insulin receptor protein expression in adipose tissue. *Am J Physiol Cell Physiol* 2003; **285**:C222-C235.